

We are IntechOpen, the world's leading publisher of Open Access books Built by scientists, for scientists

6,900

Open access books available

186,000

International authors and editors

200M

Downloads

Our authors are among the

154

Countries delivered to

TOP 1%

most cited scientists

12.2%

Contributors from top 500 universities



WEB OF SCIENCE™

Selection of our books indexed in the Book Citation Index
in Web of Science™ Core Collection (BKCI)

Interested in publishing with us?
Contact book.department@intechopen.com

Numbers displayed above are based on latest data collected.
For more information visit www.intechopen.com



Minimization of the Copper Losses in Electrical Vehicle Using Doubly Fed Induction Motor Vector Controlled

Saïd Drid

*University of Batna, Electrical Engineering Department Research Laboratory LSPIE
Algeria*

1. Introduction

The electric vehicle (EV) was conceived in the middle of the previous century. EV's offer the most promising solutions to reduce vehicular emissions. EV's constitute the only commonly known group of automobiles that qualify as zero-emission vehicles. These vehicles use an electric motor for propulsion, batteries as electrical-energy storage devices and associated with power electronics, microelectronics, and microprocessor control of motor drives.

The doubly fed induction motor (DFIM) is a wound rotor asynchronous machine supplied by the stator and the rotor from two external source voltages. This machine is very attractive for the variable speed applications such as the electric vehicle and the electrical energy production. Consequently, it covers all power ranges. Obviously, the requested variable speed domain and the desired performances depend of the application kinds (Vicatos & Tegopoulos, 2003, Akagi & Sato, 1999, Debiprasad et al., 2001, Leonhard, 1997, Wang & Ding, 1993, Morel et al., 1998 and Hopfensperger et al., 1999).

The use of DFIM offers the opportunity to modulate power flow into and out of the rotor winding in order to have, at the same time, a variable speed in the characterized super-synchronous or sub-synchronous modes in motor or in generator regimes. Two modes can be associated to slip power recovery: sub-synchronous motoring and super-synchronous generating operations. In general, while the rotor is fed through a cycloconverter, the power range can attain the MW order which presents the size power often reserved to the synchronous machine (Vicatos & Tegopoulos, 2003, Akagi & Sato, 1999, Debiprasad et al., 2001, Leonhard, 1997, Wang & Ding, 1993, Morel et al., 1998, Hopfensperger et al., 1999a, 1999b, Metwally et al., 2002, Hirofumi & Hikaru, 2002 and Djurovic et al., 1995). The DFIM has some distinct advantages compared to the conventional squirrel-cage machine. The DFIM can be controlled from the stator or rotor by various possible combinations. The disadvantage of two used converters for stator and rotor supplying can be compensated by the best control performances of the powered systems (Debiprasad et al., 2001). Indeed, the input-commands are done by means of four precise degrees of control freedom relatively to the squirrel cage induction machine where its control appears quite simple. The flux orientation strategy can transform the non linear and coupled DFIM-mathematical model into a linear model leading to one attractive solution for generating or motoring operations (Sergeial, 2003).

It is known that the motor driven systems account for approximately 65% of the electricity consumed in the world. Implementing high efficiency motor driven systems, or improving existing ones, could save over 200 billion kWh of electricity per year. This issue has become very important especially following the economic crisis due to the oil prices raising, the new energy saving technologies are appearing and developing rapidly in this century (Leonhard, 1997, Longya & Wei, 1995, Wang & Cheng, 2004, Zang & Hasan, 1999, David, 1988 and Rodriguez et al., 2002). In this framework, the DFIM continues to find great interest since the birth of the idea of the double flux orientation (Drid et al., 2005a, 2005b). The philosophy of this idea is to get a simpler machine model expression (ideal machine) (Drid et al., 2005a). Consequently, in the same time, we can solve a non linear problem presented by the DFIM control and step up from many digital simulations toward the experimental test by the use of the system dSPACE-1103. This method gives entire satisfaction and consolidates our theory, especially using the Torque Optimization Factor TOF strategy (Drid et al., 2005b). Always the search for a solution has more optimal, us nap leans towards the minimization of the copper losses in the DFIM.

In this chapter we developed an optimization factor Torque Copper Losses Optimization TCLO. The chapter will be organized as follows. The DFIM mathematical model is presented in section 3. In section 4, the robust nonlinear feedback control is exposed. Section 5 concerns the two energy torque optimization strategies TOF and TCLO. In the section 6, simulation results are exposed and comparative illustration shows the performances in energy saving between TOF and TCLO.

2. The DFIM model

Its dynamic model expressed in the synchronous reference frame is given by Voltage equations:

$$\begin{cases} \bar{u}_s = R_s \bar{i}_s + \frac{d\bar{\phi}_s}{dt} + j\omega_s \bar{\phi}_s \\ \bar{u}_r = R_r \bar{i}_r + \frac{d\bar{\phi}_r}{dt} + j\omega_r \bar{\phi}_r \end{cases} \quad (1)$$

Flux equations:

$$\begin{cases} \bar{\phi}_s = L_s \bar{i}_s + M \bar{i}_r \\ \bar{\phi}_r = L_r \bar{i}_r + M \bar{i}_s \end{cases} \quad (2)$$

From (1) and (2), the state-all-flux model is written like:

$$\begin{cases} \bar{u}_s = \frac{1}{\sigma T_s} \bar{\phi}_s - \frac{M}{\sigma T_s L_r} \bar{\phi}_r + \frac{d\bar{\phi}_s}{dt} + j\omega_s \bar{\phi}_s \\ \bar{u}_r = -\frac{M}{\sigma T_r L_s} \bar{\phi}_s + \frac{1}{\sigma T_r} \bar{\phi}_r + \frac{d\bar{\phi}_r}{dt} + j\omega_r \bar{\phi}_r \end{cases} \quad (3)$$

The electromagnetic torque is done as

$$C_e = \frac{PM}{\sigma L_s L_r} \Im m \left[\bar{\phi}_s \bar{\phi}_r^* \right] \quad (4)$$

The copper losses are giving as:

$$P_{Cl} = R_s \cdot i_s^2 + R_r \cdot i_r^2 \quad (5)$$

The motion equation is:

$$C_e - d = J \frac{d\omega}{dt} \quad (6)$$

In DFIM operations, the stator and rotor mmf's (magneto motive forces) rotations are directly imposed by the two external voltage source frequencies. Hence, the rotor speed becomes depending toward the linear combination of these frequencies, and it will be constant if they are too constants for any load torque, given of course in the machine stability domain. In DFIM modes, the synchronization between both mmf's is mainly required in order to guarantee machine stability. This is the similar situation of the synchronous machine stability problem where without the recourse to the strict control of the DFIM mmf's relative position, the machine instability risk or brake down mode become imminent.

3. Nonlinear vector control strategy

3.1 Double flux orientation

It consists in orienting, at the same time, stator flux and rotor flux. Thus, it results the constraints given below by (7). Rotor flux is oriented on the d-axis, and the stator flux is oriented on the q-axis. Conventionally, the d-axis remains reserved to magnetizing axis and q-axis to torque axis, so we can write (Drid et al., 2005a, 2005b)

$$\begin{cases} \phi_{sq} = \phi_s \\ \phi_{rd} = \phi_r \\ \phi_{sd} = \phi_{rq} = 0 \end{cases} \quad (7)$$

Using (7), the developed torque given by (4) can be rewritten as follows:

$$C_e = k_c \phi_s \phi_r \quad (8)$$

where, $k_c = \frac{PM}{\sigma L_s L_r}$

ϕ_s Appears as the input command of the active power or simply of the developed torque, while ϕ_r appears as the input command of the reactive power or simply the main magnetizing machine system acting.

3.2 Vector control by Lyapunov feedback linearization

Separating the real and the imaginary part of (3), we can write:

$$\left\{ \begin{array}{l} \frac{d\phi_{sd}}{dt} = f_1 + u_{sd} \\ \frac{d\phi_{sq}}{dt} = f_2 + u_{sq} \\ \frac{d\phi_{rd}}{dt} = f_3 + u_{rd} \\ \frac{d\phi_{rq}}{dt} = f_4 + u_{rq} \end{array} \right. \quad (9)$$

Where f_1, f_2, f_3 and f_4 are done as follows :

$$\left\{ \begin{array}{l} -f_1 = \gamma_1 \phi_{sd} - \gamma_2 \phi_{rd} - \omega_s \phi_{sq} \\ -f_2 = \gamma_1 \phi_{sq} - \gamma_2 \phi_{rq} + \omega_s \phi_{sd} \\ -f_3 = -\gamma_3 \phi_{sd} + \gamma_4 \phi_{rd} - \omega_r \phi_{rq} \\ -f_4 = -\gamma_3 \phi_{sq} + \gamma_4 \phi_{rq} + \omega_r \phi_{rd} \end{array} \right. \quad (10)$$

With:

$$\gamma_1 = \frac{1}{\sigma T_s}; \gamma_2 = \frac{M}{\sigma T_s L_r}; \gamma_3 = \frac{M}{\sigma T_r L_s}; \gamma_4 = \frac{1}{\sigma T_r}$$

Tacking into account of the constraints given by (7), one can formulate the Lyapunov function as follows

$$V = \frac{1}{2} \phi_{sd}^2 + \frac{1}{2} \phi_{rq}^2 + \frac{1}{2} (\phi_{sq} - \phi_s)^2 + \frac{1}{2} (\phi_{rd} - \phi_r)^2 > 0 \quad (11)$$

From (11), the first and second quadrate terms concern the fluxes orientation process defined in (7) with the third and fourth terms characterizing the fluxes feedback control. Where its derivative function becomes

$$\dot{V} = \phi_{sd} \dot{\phi}_{sd} + \phi_{rq} \dot{\phi}_{rq} + (\phi_{sq} - \phi_s) (\dot{\phi}_{sq} - \dot{\phi}_s) + (\phi_{rd} - \phi_r) (\dot{\phi}_{rd} - \dot{\phi}_r) \quad (12)$$

Substituting (9) in (12), it results

$$\begin{aligned} \dot{V} = & \phi_{sd} (f_1 + u_{sd}) + \phi_{rq} (f_4 + u_{rq}) + \\ & (\phi_{sq} - \phi_s) (f_2 + u_{sq} - \dot{\phi}_s) + \\ & (\phi_{rd} - \phi_r) (f_3 + u_{rd} - \dot{\phi}_r) \end{aligned} \quad (13)$$

Let us define the following law control as (Khalil, 1996):

$$\begin{cases} u_{sd} = -f_1 - K_1 \phi_{sd} \\ u_{rq} = -f_4 - K_2 \phi_{rq} \\ u_{sq} = -f_2 + \dot{\phi}_s - K_3 (\phi_{sq} - \phi_s) \\ u_{rd} = -f_3 + \dot{\phi}_r - K_4 (\phi_{rd} - \phi_r) \end{cases} \quad (14)$$

Hence (14) replaced in (13) gives:

$$\dot{V} = -K_1 \phi_{sd}^2 - K_2 \phi_{rq}^2 - K_3 (\phi_{sq} - \phi_s)^2 - K_4 (\phi_{rd} - \phi_r)^2 < 0 \quad (15)$$

The function (15) is negative one. Furthermore, (14) introduced into (9) leads to a stable convergence process if the gains K_i ($i=1, 2, 3, 4$) are evidently all positive, otherwise:

$$\begin{cases} \lim_{t \rightarrow +\infty} \phi_{sd} = 0 \\ \lim_{t \rightarrow +\infty} \phi_{rq} = 0 \\ \lim_{t \rightarrow +\infty} (\phi_{rd} - \phi_r^*) = 0 \\ \lim_{t \rightarrow +\infty} (\phi_{sq} - \phi_s^*) = 0 \end{cases} \quad (16)$$

In (16), the first and second equations concern the double flux orientation constraints applied for DFIM-model which are define above by (7), while the third and fourth equations define the errors after the feedback fluxes control. This latter offers the possibility to control the main machine magnetizing on the d-axis by ϕ_{rd} and the developed torque on the q-axis by ϕ_{sq} .

3.3 Robust feedback Lyapunov linearization control

In practice, the nonlinear functions f_i involved in the state space model (9) are strongly affected by the conventional effect of induction motor (IM) such as temperature, saturation and skin effect in addition of the different nonlinearities related to harmonic pollution due to the supplying converters and to the noise measurements. Since the control law developed in the precedent section is based on the exact knowledge of these functions f_i , one can expect that in real situation the control law (14) can fail to ensure flux orientation. In this section, our objective is to determine a new vector control law making it possible to maintain double flux orientation in presence of physical parameter variations and measurement noises. Globally we can write:

$$f_i = \hat{f}_i + \Delta f_i \quad (17)$$

On, \hat{f}_i : True nonlinear feedback function (NLFF)

f_i : Effective NLFF

Δf_i : NLFF variation around f_i .

Where: $i = 1, 2, 3$ and 4 .

The Δf_i can be generated from the whole parameters and variables variations as indicated above. We assume that all the Δf_i are bounded as follows: $|\Delta f_i| < \beta_i$; where are known bounds. The knowledge of β_i is not difficult since, one can use sufficiently large number to satisfy the constraint $|\Delta f_i| < \beta_i$.

The Δf_i can be generated from the whole parameters and variables variations as indicated above.

Replacing (17) in (9), we obtain

$$\begin{cases} \frac{d\phi_{sd}}{dt} = \hat{f}_1 + \Delta f_1 + u_{sd} \\ \frac{d\phi_{sq}}{dt} = \hat{f}_2 + \Delta f_2 + u_{sq} \\ \frac{d\phi_{rd}}{dt} = \hat{f}_3 + \Delta f_3 + u_{rd} \\ \frac{d\phi_{rq}}{dt} = \hat{f}_4 + \Delta f_4 + u_{rq} \end{cases} \quad (18)$$

The following result can be stated.

Proposition: Consider the realistic all fluxes state model (18). Then, the double fluxes orientation constraints (7) are fulfilled provided that the following control laws are used

$$\begin{cases} u_{sd} = -\hat{f}_1 - K_1 \phi_{sd} - K_{11} \operatorname{sgn}(\phi_{sd}) \\ u_{rq} = -\hat{f}_4 - K_2 \phi_{rq} - K_{22} \operatorname{sgn}(\phi_{rq}) \\ u_{sq} = -\hat{f}_2 + \dot{\phi}_s - K_3 (\phi_{sq} - \phi_s) - K_{33} \operatorname{sgn}(\phi_{sq} - \phi_s) \\ u_{rd} = -\hat{f}_3 + \dot{\phi}_r - K_4 (\phi_{rd} - \phi_r) - K_{44} \operatorname{sgn}(\phi_{rd} - \phi_r) \end{cases} \quad (19)$$

where $K_{ii} \geq \beta_i$ and $K_{ii} > 0$ for $i=1; 4$.

Proof. Let the Lyapunov function related to the fluxes dynamics (18) defined by

$$V_1 = \frac{1}{2} \phi_{sd}^2 + \frac{1}{2} \phi_{rq}^2 + \frac{1}{2} (\phi_{sq} - \phi_s)^2 + \frac{1}{2} (\phi_{rd} - \phi_r)^2 > 0 \quad (20)$$

One has

$$\begin{aligned} \dot{V}_1 = & \phi_{sd} (\Delta f_1 - K_{11} \operatorname{sgn}(\phi_{sd})) + \phi_{rq} (\Delta f_2 - K_{22} \operatorname{sgn}(\phi_{rq})) \\ & + (\phi_{sq} - \phi_s) (\Delta f_3 - K_{33} \operatorname{sgn}(\phi_{sq})) + (\phi_{rd} - \phi_r) (\Delta f_4 - K_{44} \operatorname{sgn}(\phi_{rd})) + \dot{V} < 0 \end{aligned} \quad (21)$$

where \dot{V} is given by (15). Hence the Δf_i variations can be absorbed if we take:

$$\begin{aligned}
 K_{11} > |\Delta f_1| \quad K_{11} > |\Delta f_1| \\
 K_{22} > |\Delta f_2| \quad K_{22} > |\Delta f_2| \\
 K_{33} > |\Delta f_3| \quad K_{33} > |\Delta f_3| \\
 K_{44} > |\Delta f_4| \quad K_{44} > |\Delta f_4|
 \end{aligned}
 \tag{22}$$

The latter inequalities are satisfied since $K_i > 0$ and $|\Delta f_i| < \beta_i < K_{ii}$
 Finally, we can write:

$$\dot{V}_1 < \dot{V} < 0
 \tag{23}$$

Hence, using the Lyapunov theorem (Khalil, 1996), on conclude that

$$\left\{ \begin{array}{l}
 \lim_{t \rightarrow +\infty} \phi_{sd} = 0 \\
 \lim_{t \rightarrow +\infty} \phi_{rq} = 0 \\
 \lim_{t \rightarrow +\infty} (\phi_{rd} - \phi_r^*) = 0 \\
 \lim_{t \rightarrow +\infty} (\phi_{sq} - \phi_s^*) = 0
 \end{array} \right.
 \tag{24}$$

The design of these robust controllers, resulting from (19), is given in the followed figure 2
 The indices w can be : sd, sq, rd and rq , ($i = 1,2,3$ and 4)

4. Energy optimization strategy

In this section we will explain why and what is the optimization strategy used in this work.
 Fig. 1 illustrates the problem which occurs in the proposed DFIM vector control system
 when the machine magnetizing excitation is maintained at a constant level.

4.1 Why the energy optimization strategy?

Considering an iso-torque-curve (hyperbole form), drawn from (8) for a constant torque in
 the (ϕ_s, ϕ_r) plan and lower load machine (Fig.1), on which we define two points **A** and **B**,
 respectively, corresponding to the two machine magnetizing extreme levels. Theses points
 concern respectively an excited machine ($\phi_r = 1 \text{ Wb} = \text{Const}$) and an under excited machine
 ($\phi_r = 0.1 \text{ Wb} = \text{Const}$). Both points define the steady state operation machine or equilibrium
 points. The machine rotates to satisfy the required reference speed acted by a given slope
 speed acceleration $\alpha = \frac{d\Omega}{dt} = \text{Const}$. So, the machine in both magnetizing cases must
 develop a transient torque such as:

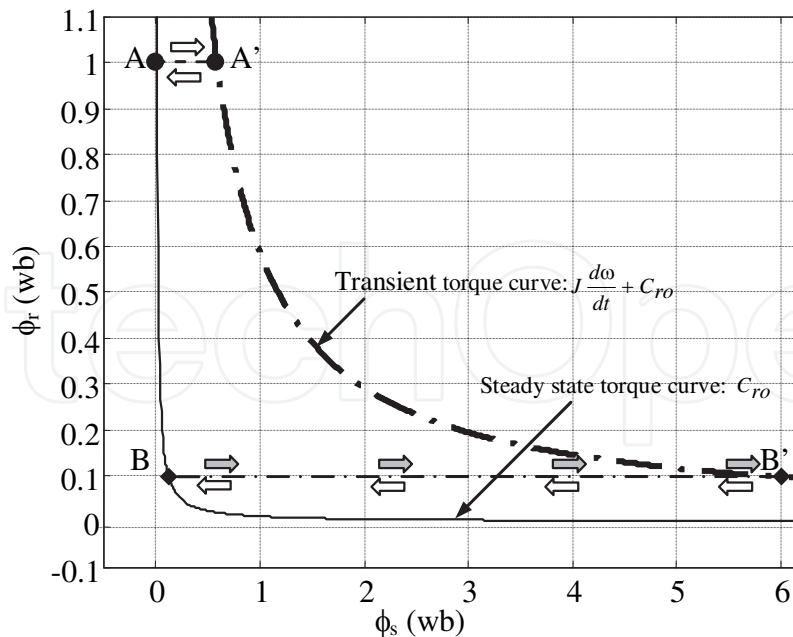


Fig. 1. Illustration of the posed problem in the DFIM control system with constant excitation.

$$C_{eT} = C_{r0} + J \frac{d\Omega}{dt} = C_{r0} + J\alpha \quad (25)$$

On the same graph, we define a second iso-torque-curve $C_{eT} = \text{Const}$ in the (ϕ_s, ϕ_r) plan. This curve is a transient one on which we place two transient points **A'** and **B'**. Here we distinguish the first transitions **A-A'** and **B-B'** due to the acceleration set, respectively for each magnetizing case. Both transitions are rapidly occurring in respect to the adopted control.

Once the machine speed reaches its reference, the inertial torque is cancelled ($\alpha = 0$), then the developed torque must return immediately to the initial load torque C_{r0} , characterized by the second transitions **A'-A** and **B'-B** towards the preceding equilibrium points **A** and **B**. One can notice that during the transition **B-B'**, corresponding to the under excited machine, the stator flux can attain very high values greater than the tolerable limit ($\phi_{s \max}$), and can tend to infinite values if the load torque C_{r0} tends to zero. So the armature currents expressed by the following formula deduced from (2) and (7) are strongly increased and can certainly destruct the machine and their supplied converters.

$$\begin{aligned} \bar{i}_s &= \lambda \cdot \phi_r + j\gamma \cdot \phi_s \\ \bar{i}_r &= \chi \cdot \phi_r + j\lambda \cdot \phi_s \end{aligned} \quad (26)$$

$$\text{Where, } \lambda = -\frac{M}{\sigma \cdot L_s \cdot L_r} \quad ; \quad \gamma = \frac{1}{\sigma \cdot L_s} \quad ; \quad \chi = \frac{1}{\sigma \cdot L_r}$$

In the other hand, for the case **A** (excited machine), if the **A-A'** transition remains tolerable, the armature currents can present prohibitory magnitude in the steady state operation due to the orthogonal contribution of stator and rotor fluxes at the moment that the machine is sufficiently excited. The steady state armature currents can be calculated by (26), where we can note the amplification effect of the coefficients λ , γ and χ .

4.2 Torque optimization factor (TOF) design

In the previous sub-section, the problem is in the transient torque, especially when the machine is low loaded. So it becomes very important to minimize the torque transition such as (Drid, 2005b):

$$\frac{dC_e}{dt} \rightarrow 0 \quad (27)$$

where,

$$dC_e = \frac{\partial C_e}{\partial \phi_s} d\phi_s + \frac{\partial C_e}{\partial \phi_r} d\phi_r \quad (28)$$

This condition should be realized respecting the stator flux constraint given by

$$\phi_s \leq \phi_{s \max} \quad (29)$$

In this way the rotor and stator fluxes, though orthogonal, their modulus will be related by the so-called TOF strategy which will be designed from the resolution of the differential equations (27-28) with constraint (29) as follows:

$$\begin{cases} \dot{\phi}_s \phi_r + \dot{\phi}_r \phi_s = 0 \\ \phi_s \leq \phi_{s \max} \end{cases} \quad (30)$$

from (29) we can write

$$-\dot{\phi}_s \phi_r = \dot{\phi}_r \phi_s \leq \dot{\phi}_r \phi_{s \max} \quad (31)$$

thus,

$$-\frac{\dot{\phi}_s}{\phi_{s \max}} \leq \frac{\dot{\phi}_r}{\phi_r} \quad (32)$$

the resolution of (32) leads to

$$-\frac{\phi_s}{\phi_{s \max}} + C \leq \ln \phi_r \quad (33)$$

where C is an arbitrary integration constant, therefore

$$\phi_r \geq e^{\left(\frac{\phi_s}{\phi_{s \max}} - C\right)} \quad (34)$$

Since, the main torque input-command in motoring DFIM operation is related to the stator flux, it becomes dependent on the speed rotor sign and thus we can write

$$\phi_{sq} = \phi_s \operatorname{sgn}(\Omega) = \begin{cases} +\phi_s & \text{if } \Omega > 0 \\ -\phi_s & \text{if } \Omega < 0 \end{cases} \quad (35)$$

with (35), (34), the rotor flux may be rewritten as follows

$$\phi_r = e \left(\frac{|\phi_{sq}|}{\phi_{s \max}} - C \right) \quad (36)$$

The resolution of (32) gives place to the arbitrary integration constant C from which the TOF-relationship (36) can be easily tuned. This one can be adjusted by a judicious choice of the integration constant, while figure 2 presents TOF effect on armature DFIM currents with C -tuning. Note that this method offers the possibility to reduce substantially the magnitude of the armature currents into the machine and we can notice an increase in energy saving. Hence using TOF strategy, we can avoid the saturation effect and reduce the magnitude of machine currents from which the DFIM efficiency could be clearly enhanced.

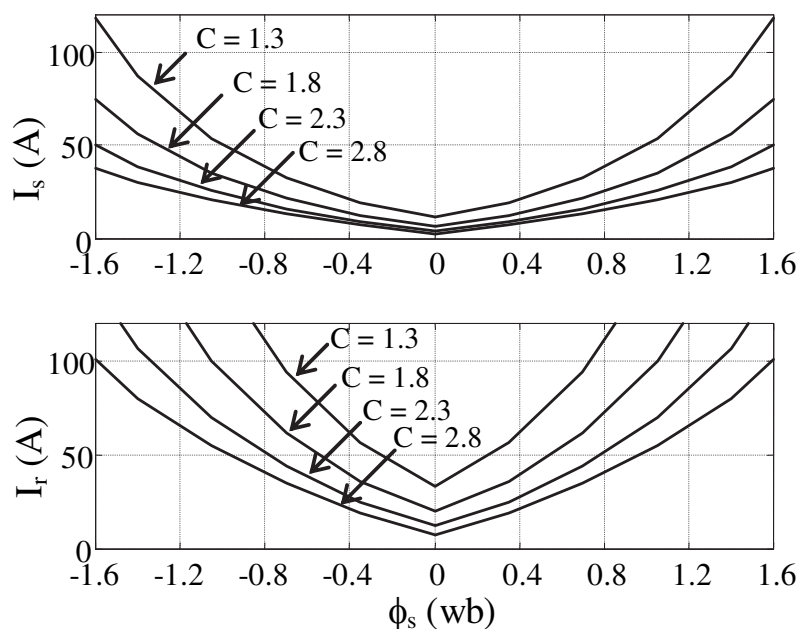


Fig. 2. TOF effect on armature DFIM currents

4.3 Torque-copper losses optimization (TCLO) design

In many applications, it is required to optimize a given parameter and the derivative plays a key role in the solution of such problems. Suppose the quantity to be minimized is given by the function $f(x)$, and x is our control parameter. We want to know how to choose x to make $f(x)$ as small as possible. Let's pick some x_0 as the starting point in our search for the best x . The goal is to find the relation between fluxes which can optimize the compromise between torque and copper losses in steady state as well as in transient state, (i.e. for all $\{C_e\}$ find (ϕ_s, ϕ_r) let $\min\{P_{cl}\}$) (Drid, 2008). From (5), (8) and (26), the torque and copper losses can be to written as:

$$\begin{cases} C_e = k_c \cdot \phi_r \cdot \phi_s \\ P_{cl} = a_1 \phi_r^2 + a_2 \phi_s^2 \end{cases} \quad (37)$$

$$a_1 = \left(\frac{R_r}{(\sigma \cdot L_r)^2} + \frac{R_s M^2}{(\sigma \cdot L_r \cdot L_s)^2} \right)$$

with :

$$a_2 = \left(\frac{R_r M^2}{(\sigma \cdot L_r \cdot L_s)^2} + \frac{R_s}{(\sigma \cdot L_s)^2} \right)$$

The figure 3 represents the layout of (37) for a constant level of torque and copper losses in the (ϕ_s, ϕ_r) plan. These curves present respectively a hyperbole for the iso-torque and ellipse for iso-copper-losses. From (37) we can write:

$$a_1 k_c^2 \phi_r^4 - k_c^2 \phi_r^2 \Delta P_{cl} + a_2 C_{el}^2 = 0 \tag{38}$$

To obtain a real and thus optimal solution, we must have:

$$\Delta = k_c^4 \Delta P_{cl}^4 - 4a_1 k_c^2 a_2 C_{el}^2 = 0 \tag{39}$$

The equation (39) represents the energy balance in the DFIM for one working DFIM point as shown in fig.3. Then, one can write:

$$\Delta P_{cl} = \sqrt{\frac{4a_1 a_2 C_{el}^2}{k_c^2}} \tag{40}$$

This equation shows the optimal relation between the torque and the copper losses.

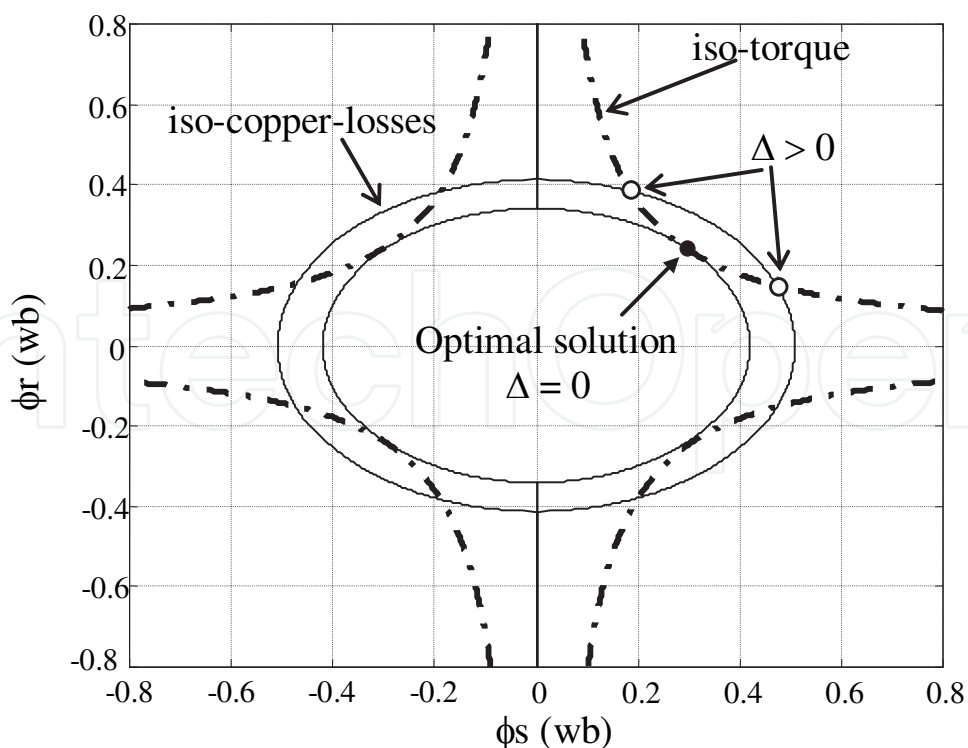


Fig. 3. The iso-torque curves and the iso-losses curves in the plan (ϕ_s, ϕ_r)

4.4 Finding minimum Copper-losses values

The Rolle's Theorem is the key result behind applications of the derivative to optimization problems. The second derivative test is used to finding minimum point.

We can rewrite (37) as:

$$\begin{cases} \phi_s = \frac{C_e}{k_c \cdot \phi_r} \\ P_{cl} = a_1 \phi_r^2 + a_2 \frac{C_e^2}{k_c^2 \cdot \phi_r^2} = \frac{a_1 k_c^2 \phi_r^4 + a_2 C_e^2}{k_c^2 \cdot \phi_r^2} \end{cases} \quad (41)$$

The computations of the first and second derivatives show that the critical point is given by:

$$\phi_{rc} = \pm \left(\frac{C_e^2 a_2}{a_1 k_c^2} \right)^{\frac{1}{4}} \quad (42)$$

For which:

$$\frac{d^2 P_{cl}(\phi_{rc})}{d\phi_r^2} = \frac{2a_1 k_c^2 \phi_{rc}^4 + 6a_2 C_e^2}{k_c^2 \cdot \phi_{rc}^4} = 8a_1 > 0 \quad (43)$$

We can see that the second derivative is positive and conclude that the critical point is a relative minimum.

5. Simulation

Figure 4 illustrates a general block diagram of the suggested DFIM control scheme. Here, we can note the placement of optimization block, the first estimator-block which evaluates torque and the second estimator-block which evaluates firstly the modulus and position fluxes, respectively ϕ_s , ϕ_r , ρ_s and ρ_r , from the measured currents using (2) and secondly the feedback functions f_1 , f_2 , f_3 , f_4 given by (10). Optimization process allows adapting the main flux magnetizing defined by rotor flux to the applied load torque characterized by the stator flux. With the analogical switch we can select the type of the reference rotor flux. The switch position 1, 2 gives respectively TCLO and TOF for optimized operation and the position 3 for a magnetizing constant level.

The Figure 5 shows the speed response versus time according to its desired profile drawn on the same figure. Figure 6 illustrate the fluxes trajectory of the closed-loop system. It moves along manifold toward the equilibrium point. We can notice the stability of the system. Figures 7 and 8 show respectively the stator and the rotor input control voltages versus time during the test. Figure 9 present the copper losses according to the stator flux variations in steady state operation and we can see the contribution of the TCLO compared to the TOF. Finally figure 10 present the dissipated energy versus time from which we can observe clearly the influence of the three switch positions on the copper losses in transient state. We can conclude that the TCLO is the best optimization.

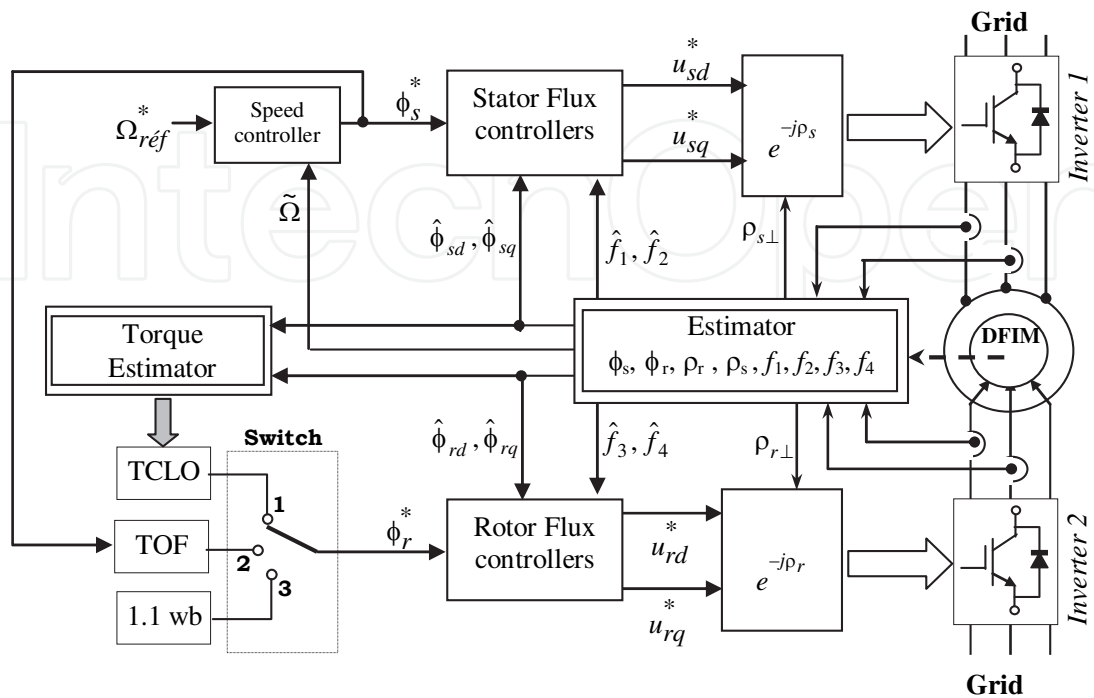


Fig. 4. General block diagram of control scheme

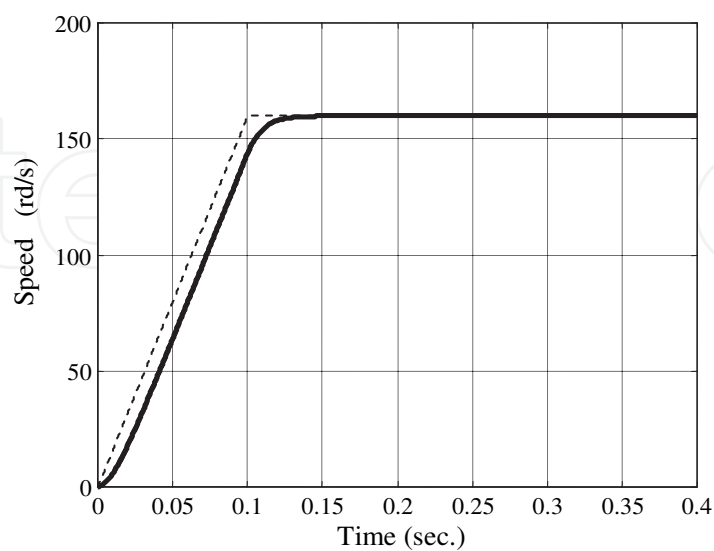


Fig. 5. Speed response

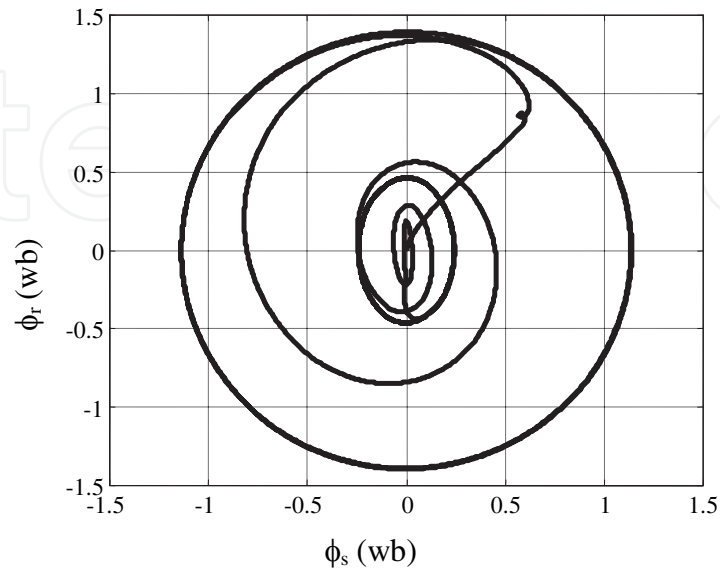


Fig. 6. Fluxes trajectories of the closed-loop system

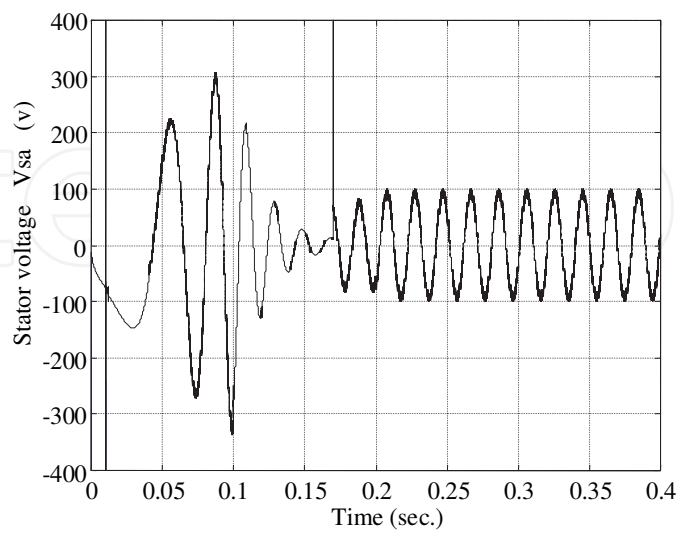


Fig. 7. The input control stator voltage response in the stator reference frames with TCLO

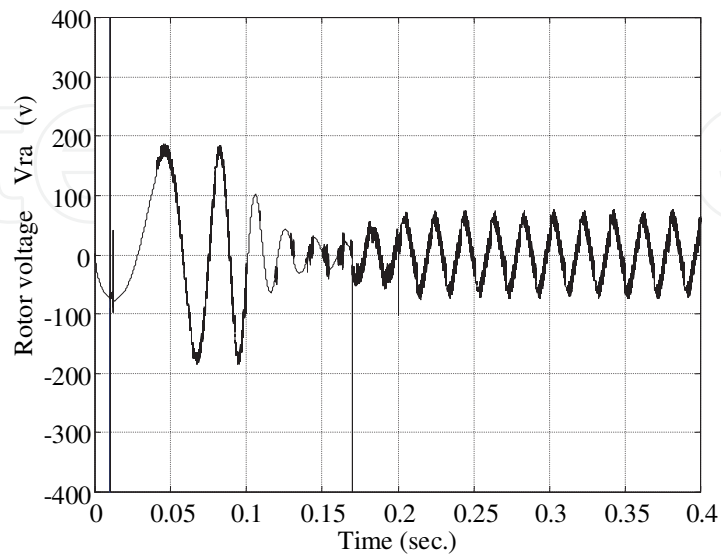


Fig. 8. The input control rotor voltage response in the stator reference frames with TCLO

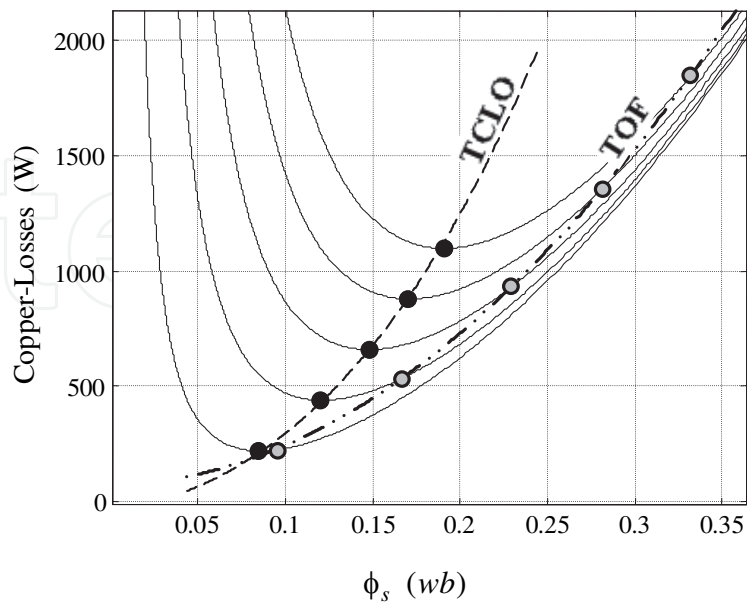


Fig. 9. Minimized copper losses in steady state operation with TOF and TCLO

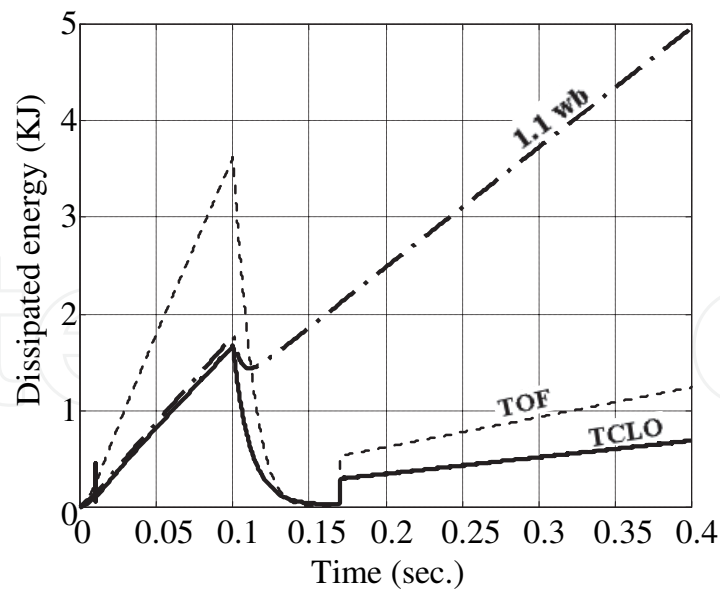


Fig. 10. Total copper losses versus time during test for the three switch positions (Energy saving illustration)

6. Conclusion

In this chapter was presented a vector control intended for doubly fed induction motor (DFIM) mode. The use of the state-all-flux induction machine model with a flux orientation constraint gives place to a simpler control model. The stability of the nonlinear feedback control is proven using the Lyapunov function.

The simulation results of the suggested DFIM system control based on double flux orientation which is achieved by the proposed DFIM control demonstrates clearly the suitable obtained performances required by the references profiles defined above. The speed tracks its desired reference without any effect of the load torque. Therefore the high control performances can be well affirmed. To optimize the machine operation we chose to minimize the copper losses. The proposed TCLO factor performs better than the already designed TOF. Indeed, the energy saving process can be well achieved if the magnetizing flux decreases in the same way as the load torque. It results in an interesting balance between the core losses and the copper losses into the machine, so the machine efficiency may be largely improved. The simulation results confirm largely the effectiveness of the proposed DFIM control system.

7. Appendix

The machine parameters are:

$R_s = 1.2 \Omega$; $L_s = 0.158 \text{ H}$; $L_r = 0.156 \text{ H}$; $R_r = 1.8 \Omega$; $M = 0.15 \text{ H}$; $P = 2$; $J = 0.07 \text{ Kg.m}^2$; $P_n = 4 \text{ Kw}$; $220/380\text{V}$; 50Hz ; 1440tr/min ; $15/8.6 \text{ A}$; $\cos\phi = 0.85$.

8. Nomenclature

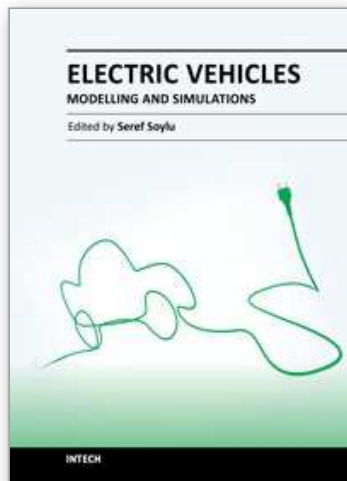
- s, r Rotor and stator indices.
 d, q Direct and quadrature indices for orthogonal components
 \bar{x} Variable complex such as: $\bar{x} = \Re[\bar{x}] + j \cdot \Im[\bar{x}]$.

\bar{x}	It can be a voltage as \bar{u} , a current as \bar{i} or a flux as $\bar{\phi}$
\bar{x}^*	Complex conjugate
R_s, R_r	Stator and rotor resistances
L_s, L_r	Stator and rotor inductances
T_s, T_r	Stator and rotor time-constants ($T_{s,r} = L_{s,r} / R_{s,r}$)
σ	Leakage flux total coefficient ($\sigma = 1 - M^2 / L_r L_s$)
M	Mutual inductance
θ	Absolute rotor position
p	Number of pairs poles
δ	Torque angle
ρ_s, ρ_r	Stator and rotor flux absolute positions
ω	Mechanical rotor frequency (rd/s)
Ω	Rotor speed (rd/s)
ω_s	Stator current frequency (rd/s)
ω_r	Induced rotor current frequency (rd/s)
J	Inertia
d	Unknown load torque
C_e	Electromagnetic torque
\sim	Symbol indicating measured value
\wedge	Symbol indicating the estimated value
$*$	Symbol indicating the command value
DFIM	Doubly Fed Induction Machine
TOF	Torque Optimization Factor
TCLO	Torque Copper Losses Optimization

9. References

- Vicatos, M.S. & Tegopoulos, J. A. (2003). A Doubly-Fed Induction Machine Differential Drive Model for Automobiles, *IEEE Transactions on Energy Conversion*, Vol.18, No.2, (June 2003), pp. 225-230, ISSN 0885-8969
- Akagi, H. & Sato, H. (1999). Control and Performance of a Flywheel Energy Storage System Based on a Doubly-Fed Induction Generator-Motor, *Proceedings of the 30th IEEE Power Electronics Specialists Conference*, pp. 32-39, vol1, ISBN 0275-9306, Charleston, USA, 27 June-1 July, 1999
- Debiprasad, P. et al (2001). A Novel Control Strategy for the Rotor Side Control of a Doubly-Fed Induction Machine. *IEEE Industry Applications Conference and Thirty-Sixth IAS Annual Meeting*, pp. 1695-1702, ISBN: 0-7803-7114-3, Chicago, USA, 30 September-04 October 2001
- Leonhard, W. (1997). *Control Electrical Drives*, Springer verlag, ISBN 3540418202, Berlin Heidelberg, Germany
- Wang, S. & Ding, Y. (1993). Stability Analysis of Field Oriented doubly Fed induction Machine drive Based on Computed Simulation, *Electrical Machines and Power Systems*, Vol. 21, No. 1, (1993), pp. 11-24, ISSN 1532-5008
- Morel, L. et al. (1998). Double-fed induction machine: converter optimisation and field oriented control without position sensor, *IEE proceedings Electric power applications*, Vol. 145. No. 4, (July 1998), pp. 360-368, ISSN 1350-2352

- Hopfensperger, B. et al., (1999) Stator flux oriented control of a cascaded doubly fed induction machine, *IEE proceedings Electric power applications*, Vol. 146. No. 6, (November 1999), pp. 597-605, ISSN 1350-2352
- Hopfensperger, B. et al., (1999) "Stator flux oriented control of a cascaded doubly fed induction machine with and without position encoder, *IEE proceedings Electric power applications*, Vol. 147. No. 4, (July 1999), pp. 241-250, ISSN 1350-2352
- Metwally, H.M.B. et al. (2002). Optimum performance characteristics of doubly fed induction motors using field oriented control, *Energy conversion and Management*, Vol. 43, No. 1, (2002), pp. 3-13, ISSN 0196-8904
- Hirofumi, A. & Hikaru, S. (2002). Control and Performance of a Doubly fed induction Machine Intended for a Flywheel Energy Storage System, *IEEE Transactions on Power Electronics*, Vol. 17, No. 1, (January 2002), pp. 109-116, ISSN 0885-8993
- Djurovic, M. et al. (1995). Double Fed Induction Generator with Two Pair of Poles, *IEE Conferences of Electrical Machines and Drives*, pp. 449-452, ISBN 0-85296-648-2, Durham, UK, 11-13 September 1995
- Leonhard, W. (1988). Adjustable-Speed AC Drives, Invited Paper, *Proceedings of the IEEE*, vol. 76, No. 4, (April 1988), pp.455-471. ISSN 0018-9219
- Longya, X. & Wei C. (1995). Torque and Reactive Power control of a Doubly Fed Induction Machine by Position Position Sensorless Scheme. *IEEE Transactions on Industry Applications*, Vol. 31, No. 3, (May/June 1995), pp 636-642 ISSN 0093-9994
- Sergei, P., Andrea, T. & Tonielli, A. (2003). Indirect Stator Flux-Oriented Output Feedback Control of a Doubly Fed Induction Machine, *IEEE Trans. On control Systems Technology*, Vol. 11, No. 6, (Nov. 2003), pp. 875-888, ISSN 1063-6536
- Wang, D.H. & Cheng, K.W.E. (2004). General discussion on energy saving Power Electronics Systems and Applications. *Proceedings of the First International Conference on Power Electronics Systems and Applications*, pp298-303, ISBN 962-367-434-1, USA, 9-11 Nov. 2004
- Zang, L. & Hasan K.H, (1999). Neural Network Aided Energy Efficiency control for a Field Orientation Induction Machine Drive. *Proceeding of Ninth International conference on Electrical Machine and Drives*, pp. 356-360, ISSN 0537-9989, Canterbury, UK, 1-3 September 1999
- David, E. (1988). A Suggested Energy-Savings Evaluation Method for AC Adjustable-Speed Drive Applications," *IEEE Trans. on Industry Applications*, Vol. 24, No. 6, (Nov/Dec. 1988), pp1107-1117, ISSN 0093-9994
- Rodriguez, J. et al. (2002). Optimal Vector Control of Pumping and Ventilation Induction Motor Drives. *IEEE Trans. on Electronics Industry*, vol. 49, No. 4, (August 2002), pp.889-895, ISSN 0278-0046
- Drid, S., Nait_Said, M.S. & Tadjine, M. (2005). Double flux oriented control for the doubly fed induction motor. *Electric Power Components & Systems Journal*, Vol. 33, No.10, (October 2005), pp. 1081-1095, ISSN 1532-5008
- Drid, S., Tadjine, M. & Nait_Said, M.S. (2005). Nonlinear Feedback Control and Torque Optimization of a Doubly Fed Induction Motor. *JEEEC Journal of Electrical Engineering Elektrotechnický časopis*, vol. 56, No. 3-4, (2005), pp. 57-63, ISSN 1335-3632
- Drid, S., Nait-Said, M.S., Tadjine M. & Makouf A.(2008), Nonlinear Control of the Doubly Fed Induction Motor with Copper Losses Minimization for Electrical Vehicle, *CISA08, 1st Mediterranean Conference on Intelligent Systems and Automation, AIP Conf. Proc.*, Vol. 1019, pp.339-345, Annaba, Algeria, June 30-July 02, 2008
- Khalil, H., (1996), Nonlinear systems. Prentice Hall, ISBN 0-13-067389-7, USA



Electric Vehicles - Modelling and Simulations

Edited by Dr. Seref Soylu

ISBN 978-953-307-477-1

Hard cover, 466 pages

Publisher InTech

Published online 12, September, 2011

Published in print edition September, 2011

In this book, modeling and simulation of electric vehicles and their components have been emphasized chapter by chapter with valuable contribution of many researchers who work on both technical and regulatory sides of the field. Mathematical models for electrical vehicles and their components were introduced and merged together to make this book a guide for industry, academia and policy makers.

How to reference

In order to correctly reference this scholarly work, feel free to copy and paste the following:

Säid Drid (2011). Minimization of the Copper Losses in Electrical Vehicle Using Doubly Fed Induction Motor Vector Controlled, *Electric Vehicles - Modelling and Simulations*, Dr. Seref Soylu (Ed.), ISBN: 978-953-307-477-1, InTech, Available from: <http://www.intechopen.com/books/electric-vehicles-modelling-and-simulations/minimization-of-the-copper-losses-in-electrical-vehicle-using-doubly-fed-induction-motor-vector-cont>

INTECH
open science | open minds

InTech Europe

University Campus STeP Ri
Slavka Krautzeka 83/A
51000 Rijeka, Croatia
Phone: +385 (51) 770 447
Fax: +385 (51) 686 166
www.intechopen.com

InTech China

Unit 405, Office Block, Hotel Equatorial Shanghai
No.65, Yan An Road (West), Shanghai, 200040, China
中国上海市延安西路65号上海国际贵都大饭店办公楼405单元
Phone: +86-21-62489820
Fax: +86-21-62489821

© 2011 The Author(s). Licensee IntechOpen. This chapter is distributed under the terms of the [Creative Commons Attribution-NonCommercial-ShareAlike-3.0 License](#), which permits use, distribution and reproduction for non-commercial purposes, provided the original is properly cited and derivative works building on this content are distributed under the same license.

IntechOpen

IntechOpen